THE DEGREE AND THE MECHANISM OF SKIN FRICTION REDUCTION BY MICROBUBBLES

Yoshiaki Kodama, Kazuyasu Sugiyama, Atsuhide Kitagawa, Masahiko Makino, Takahito Takahashi
Center for Smart Control of Turbulence,
National Maritime Research Institute
Shinkawa, Mitaka, Tokyo 181-0004, Japan
kodama@nmri.go.jp, sugiyama@nmri.go.jp, kitagawa@nmri.go.jp, makino@nmri.go.jp, takahito@nmri.go.jp

Koichi Hishida,
Department of System Design Engineering,
Keio University
Hiyoshi, Kohoku-ku, Yokohama, Kanagawa 223-8522, Japan
hishida@sd.keio.ac.jp

Shu Takagi
Department of Mechanical Engineering,
The University of Tokyo
Hongo, Bunkyo-ku, Tokyo 113-8656, Japan
takagi@mech.t.u-tokyo.ac.jp

ABSTRACT

First the applicability of microbubbles to ships as a skin friction reduction device is reviewed on their efficiency and from the environmental viewpoint, based on some experimental results including full scale. The review result is mostly favorable, but it is commented that the skin friction reduction mechansim is still unclear. Then two resutls of the most recent research on the skin friction reduction mechanism are shown in detail. One is an experimental one, in which microbubble flow was optically measured and the reduction of the Reynolds stress by microbubbles was obtained. The other is a numerical one, in which bubble injection into a turbulent channel flow was simulated and skin friction reduction was obtained. Finally some discussions on the skin friction reduction mechanism are given.

INTRODUCTION

Since the pioneering work by McCormick and Bhattacharyya (1973), microbubbles, i.e. small air bubbles injected into the turbulent boundary layer developing along the solid surface of a body moving in water, are known to have significant skin friction reduciton effect (e.g. Merkle and Deutsch 1990). Further, microbubble experiments using long flat plates towed in towing tanks at cruising speed of large ships have shown that the skin friction reduction effect persists for more than 40m in the downstream direction after injection (Watanabe et al. 1998, Takahashi et al. 2001, Takahashi et al. 2003). Therefore microbubbles are regarded as a promising drag reduction device applicable to ships, and intensive studies have been carried out (e.g. Kodama et al. 2002a). Recently the drag reduction effect of microbubbles was confirmed in a full-scale experiment using a 116m-long ship (Kodama et al. 2002b, Nagamatsu et al. 2002).

Fig.1 shows an image of the apllication of microbubbles to a tanker ship. Large ships such as tankers, which play an important role in the global transport, have a box shape with a wide and flat bottom. Such a shape is suitable for microbubbles, because if bubbles are injected at bow, buoyancy will help them to stay close to the bottom wall and thus help them to cover efficiently the entire bottom surface. Microbubbles are expected to have better drag reduction efficiency on larger ships, because of the long persisitence of the skin friction reduction effect confirmed by the experiments using long flat plates. Further, recent regulations demand that large tankers have double hull structure to prevent oil spilling in case of accidents such as gounding, and therefore microbubbles devices can be easily installed in such ships.

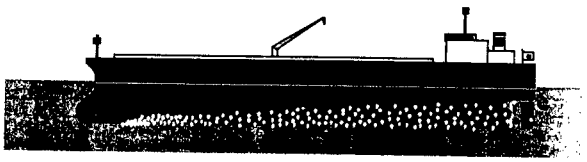

Figure 1 An image of microbubbles applied to a tanker ship

In order to discuss the applicability of microbubbles to ships, it is necessary to take into account the power needed to inject bubbles against the hydrostatic pressure. The water depth of a large tanker at full load is approximately 20m, and therefore the power needed is not nominal. However the skin friction reduction already obtained is so large that Kodama et al. (2002a) have estimated 5% net power saving by microbubbles on a ship of 100m length and 7m water depth, based on the 50m-long flat plate data. One way to further reduce the needed power is to utilize the flow around a ship hull, which generally directs downward while it goes from the bow to the middle . In the full-scale experiment (Nagamatsu et al. 2002), where the water depth was 5.7m, air bubbles were injected at the 1m water depth location in the bow part. In that case 3%

drag reduction was obtained, and the power needed for bubble injection was estimated to be 1% by taking into account the hydrostatic pressure at injection point, and therefore 2% net power-saving was obtained.

One of the advantages of microbubbles is that it is environmentally friendly, in contrast to other skin friction devices having significant skin friction reduction effect, such as polymers or surfactants. It is hard to think that air bubbles injected into sea water cause harm. Kanai et al. (2001) have proposed an interesting way to discharge CO_2 contained in the exhaust gas from engines directly into sea water, by using the exhaust gas for microbubble generation. They report that more than 60% of CO_2 included in the exhaust gas is easily dissolved into sea water while the bubbles travel along the hull surface. Thus one could get drag reduction and the reduction of CO_2 emission into air simultaneously. This method is not free from pollution problems because water with dissolved CO_2 is weakly acid and exhaust gas contains hazardous substance. But they do not necessarily mean that this method increases pollution, because exhaust gas is hazardous by itself and is emitted into air otherwise.

The understanding on the basic mechanism of the skin friction reduction effect of microbubbles is not yet fully established, in spite of its significant reduction effect and the long research history, mainly because the existence of bubbles itself prevents detailed study, either experimental or theoretical. This fact imposes a serious handicap on the practical application of microbubbles, because any engineering device cannot be assuredly put to practice without knowing its physical mechanism.

A research project called "The Smart Control of Turbulence ; A Millennium Challenge for Innovative Thermal and Fluids Systems" has started in 2000 as a five-year project funded by the Ministry of Education, Culture, Sports, Science and Technology of the Japanese government (Kasagi and Kodama 2000). In the project, microbubbles are studied with a focus on elucidating the skin friction reduction mechanism. In the following chapters, some recent results of the study are shown.

MEASUREMENT OF MICROBUBBLE FLOW USING PTV/LIF/IST

Kitagawa et al. (2003) measured turbulence properties of microbubble flows using a PTV/LIF/IST (Particle Tracking Velocimetry / Laser-Induced Fluorescence / Infrared Shadow Technique) technique, in a circulating water tunnel shown in Fig. 2, whose test section has size $L_c \times B_c \times H_c$ = 3000mm × 100mm × 15mm. Air was injected through an Array-of-Holes plate (AHP), with 0.5mm diameter holes drilled at 2.5mm streamwise and 1.9mm spanwise pitches in an area of L_a =36mm and B_a =72mm, located at 1038mm from the upstream edge of the test section. The measurement was carried out at 464mm from the downstream edge of the injection plate and at the bulk flow speed U_∞ =5m/s. Laser-fluorescent tracer particles were added to the water. Fig. 3 shows the PTV/LIF/IST device, which enables simultaneous measurement of flow velocity and bubble motion. A laser light sheet is emitted into the test section from the bottom wall. Two facing mirrors set at 45 degrees on the top wall are used to shorten the light path and thus to improve visibility. The LIF light emitted from tracer particles is reflected first by a mirror and then by a cold mirror before going into the CCD camera. The laser light reflected from bubbles is cut off by a color filter attached to the camera. Infra-red light is emitted from the LED array on the top wall, reflected twice by the mirrors, color-separated by the cold mirror, and then goes into another CCD camera.

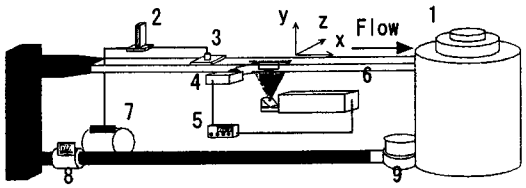

1: Dump tank
2: Mass flow controller
3: Air injection region
4: CCD Camera
5: Pulse generator
6: YAG Laser
7: Air compressor
8: Electro magnetic flow meter
9: Pump

Figure 2 A circulating water tunnel for microbubble measurement using PTV/LIF (Kitagawa et al. 2003)

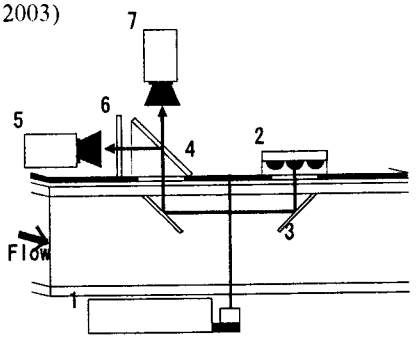

1: YAG Laser
2: LED array
3: Mirror
4: Cold mirror
5: CCD Camera for PTV/LIF
6: Color filter
7: CCD Camera for bubbles

Figure 3 PTV/LIF/IST device in a circulating water tunnel (Kitagawa et al. 2003).

Fig. 4 shows an example of PTV/LIF result. Fig.4(a) shows bubble images, and Fig.4(b) shows an overlap of the analyzed bubble images and velocity vectors from PTV taken at the same instant. Originally, PIV was used for the analysis (Nagaya et al. 2002), but it has been found out that the bubble images cannot be removed coompletely, and therefore it has been switched to PTV. Using this technique, it is possible to obtain bubble motion/deformation information and velocity field information of the liquid phase simultaneously and in complete separation. Since the IST part is currently preliminary, only the PTV part is described in detail in what follows.

Fig. 5 shows the PTV results. Fig. 5(a) shows the mean U velocity component. α denotes the bulk void ratio in the test section defined as

$$\alpha \equiv \frac{Q_a}{Q_w + Q_a}, \qquad (1)$$

where Q_a is the injected air flow rate and Q_w is the water flow rate. The horizontal axis shows the distance from the wall y, normalized by the channel half height h. Using Dean's equation for rectangular duct flow (Dean 1978), the friction velocity at U_∞ =5m/s is estimated to be U_τ =0.2416m/s. Using this value,

y/h =0.1 corresponds to y^+ =180. Near the wall, U becomes slightly smaller with increasing α. The figure also shows the logarithmic curve of the form

$$\frac{U}{U_\tau} = 5.5\log_{10}\frac{U_\tau y}{\nu} + 5.4, \qquad (2)$$

where the friction velocity U_τ has been obtained by least square fitting the curve to the data at $y^+ < 700$. The U_τ at α =0% thus obtained is U_τ =0.2366m/s, which agrees with that obtained by Dean's equation with 2% discrepancy. The y-component V was $|V| \le 0.01 m/s$, i.e. almost zero everywhere.

Fig. 5(b) shows the local skin friction reduction measured using a skin friction sensor of the force balance type. No wall effect correction (Kodama et al. 2000) has been applied. The z value denotes the spanwise distance from the channel axis. The skin friction reduction estimated by the least square fit as shown in Fig.5(a) is also plotted. The z=0mm values show some scatter, and the estimated least square fit values agree well with the values measured at z=-25mm.

Fig. 5(c) shows the RMS values of the fluctuating velocity components. Both components increase, not in the vicinity of the wall but somewhat away from it, as α increases.

Fig. 5(d) shows the Reynolds shear stress, which, in spite of the increase of the fluctuating velocity components, decreases as α increases, which is in agreement with the skin friction reduction shown in Fig. 5(b). Again, the reduction of the Reynolds stress occurs not in the vicinity of the wall but somewhat away from it.

Fig. 5(e) shows the local void ratio distribution at U_∞ =5m/s, α =8%, using AHP with 1mm diameter holes drilled at 3mm and 5mm pitches in an area of 72mm × 72mm, measured with a suction tube system (Kodama et al. 2000). Although the condition is not the same as that of Figs. 4(a) - (d), it give some idea on the corresponding distribution. The high local void ratio zone roughly agrees with the zone of increased fluctuating velocity components .

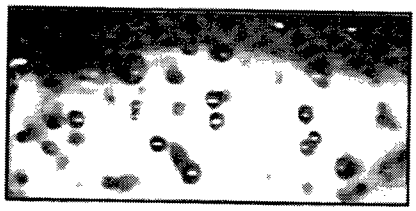

(a)Bubble image

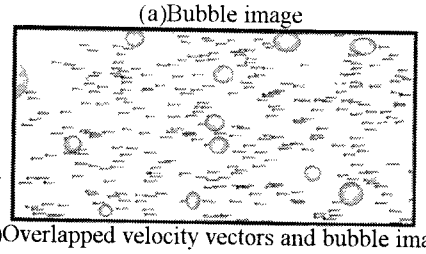

(b)Overlapped velocity vectors and bubble images

Figure 4 Bubble images and velocity vectors obtained using PTV/LIF (Kitagawa et al. 2003)

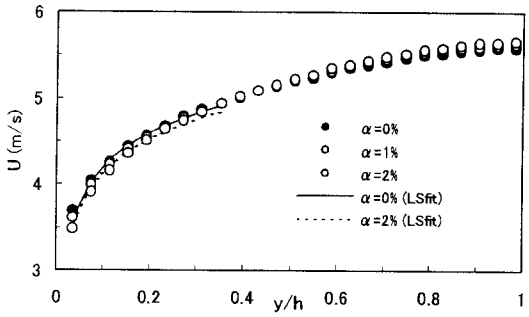

(a)Mean velocity U

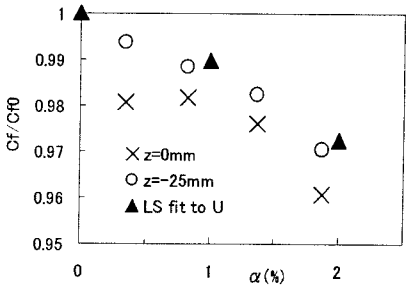

(b) Local skin friction reduction

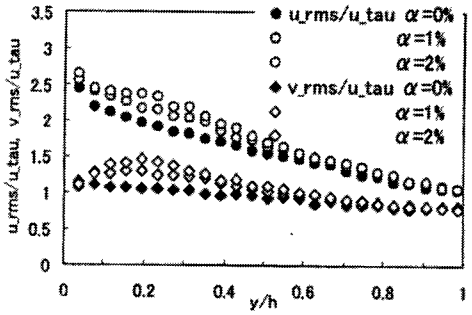

(c) Fluctuating velocities

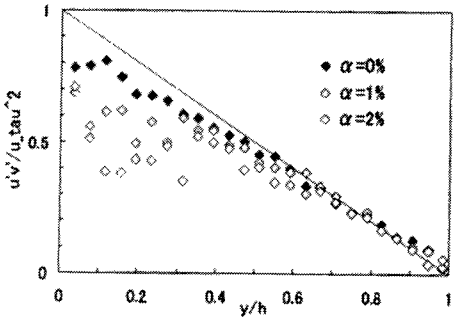

(d)Reynolds stress

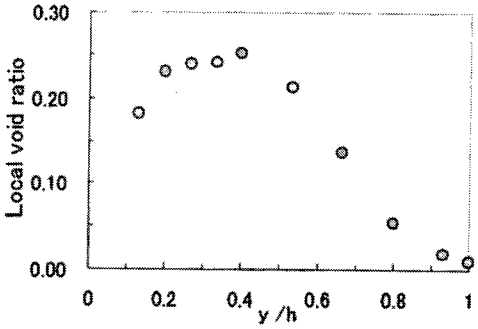

(e)Local void ratio (α =8%)

Figure 5 Turbulence measurement using PTV/LIF (Kitagawa et al. 2003)

NUMERICAL SIMULATION OF MICRO-BUBBLE FLOW USING THE EULERIAN-LAGRANGIAN METHOD

Sugiyama et al. (2003) simluated microbubble flows using the EL (Eulerian-Lagrangian) method, in which the liquid phase is computed in the Eulerian way and the bubble motion is computed in the Lagrangian way. The equation for bubble motion is

$$\frac{d\vec{u}_G}{dt} = \frac{1}{St}(\vec{u}_L - \vec{u}_G)(1+0.15\mathrm{Re}_b^{0.687}) + 3\left\{\frac{d\vec{u}_L}{dt} + (\vec{u}_L \cdot \nabla)\vec{u}_L\right\} \quad (3)$$

where the subscripts L and G denote liquid and gas phases respectively, St is the Stokes number, and Re_b is the bubble Reynolds number. The first term on the righthand side represents drag, and the second term represents inertia. The buoyancy effect is not included.

Two cases were computed.

Periodic case

A perirodic boundary condition was used in the streamwise direction. The streamwise pressure gradient was kept constant. Initially, bubbles were distributed either uniformly or non-uniformly as shown in Table 1. f_{G0}, the bulk void fraction in the entire domain, was kept constant, which means that the total bubble volume is the same in the three cases, and the degree of clustering toward the top wall increases as the case number increases. The size of the computational domain is $2\pi h$ (length)$\times$ $2h$ (height)$\times$ πh (width) containing $64\times64\times64$ grid points. The Reynolds number based on friction velocity and channel half height is Re_τ=150. Non-dimensional bubble diameter is d^+=2. The Stokes number is St=0.1.

Fig. 6 shows the temporal evolution of relative skin friction coefficient, in which C_{f0} denotes that in single phase. In the uniform distribution case there is almost no skin friction reduction. In the non-uniform cases the skin friction reduces, and the degree of reduction is larger when bubbles are initially more clustered toward the wall. Xu et al. (2002) also carried out computations of initially clusered microbubbles using periodic boundary conditions, and obtained skin friction reduction.

Table 1 Initial bubble distribution

Case	f_{G0} (%)	Initial bubble location
1	0.1	$0<y^+<300$ (uniform)
2	0.1	$0<y^+<20$ (non-uniform)
3	0.1	$0<y^+<10$ (non-uniform)

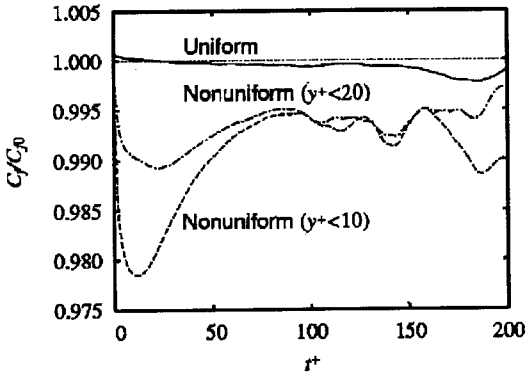

Figure 6 Temporal evolution of relative skin friction coeffficient on top wall (Periodic case) (Sugiyama et al. 2003).

Non-periodic case

In order to simulate persistence of the skin friction reduction effect of microbubbles in the downstream direction, Sugiyama et al. (2003) also carried out computations of the non-periodic case. As shown in Fig. 7, the computational domain is divided into two. One is the upstream zone, in which a fully developed turbulent flow of single phase was computed using periodic streamwise boundary conditions. The size of the zone is $2\pi h$ (length) $\times$ $2h$ (height) $\times$ πh (width) containing $64\times64\times64$ grid points. The other is the downstream zone. The size of the zone is 10 πh (length) $\times$ 2 h (height) $\times$ πh (width) containing 320 $\times$ 64 $\times$ 64 grid points. Bubbles were injected from the top wall, in the region $\pi/2 \le x/h \le \pi$, where $x=0$ corresponds to the upstream boundary. At the upstream boundary, velocity and pressure values computed in the upstream zone were imposed as Dirichlet conditions. The Neumann boundary condtions were imposed at the downstream boundary. f_{G0} was set at 0.3%. Bouyancy was not included in the results shown here.

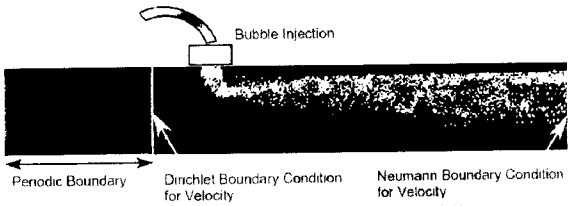

Figure 7 Boundary conditions in the non-peridic case (Sugiyama et al. 2003).

The computed flow is visualized in Fig. 8. Fig. 9(a) shows the skin friction on top and bottom walls. They have been averaged in the time interval between t^+=1500 and 15000. At the top wall, the skin friction reduces not only at downstream of injection but also at upstream. The reduction persists longer than x/h=25. The reduction can be explained by the difference of velocity vectors in the bubble and non-bubble conditions shown in Fig. 9(b). Near the top wall the relative velocities has negative streamwise components, and near the bottom wall they are slightly positive. These tendencies agree well with those in the skin friction distribution.

The normalized stress balance equation in x-direction is written as

$$\nu\frac{\partial\overline{u_L}}{\partial y} - \int_0^y \frac{\partial\overline{f_L u_L u_L}}{\partial x}dy - \overline{f_L u_L v_L} - \int_0^y \frac{\partial\overline{p}}{\partial x}dy = 1 - \frac{y}{h} \quad (4)$$

The magnitude of the terms of LHS at $0.79h$ distance from the downstream end of the injection zone is plotted in Fig. 9(c). The magnitude of the first term at the top wall is slightly less than that of the total, showing skin friction reduction. The pressure gradient term, i.e. the 4th term, seems responsible for the reduction. The magnitude of the third term mostly exceeds that of the total. This looks in disagreement with the measured Reynolds stress shown in Fig.4(d), but it should be noticed that the third term of eq.(4) includes contribution from mean velocities, which should be subtracted in order to compare directly with the measured Reynolds stress, as Sugiyama et al. (2003) did.

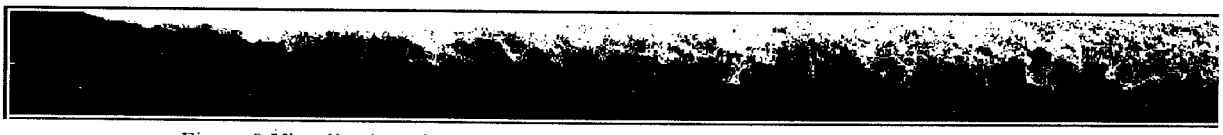

Figure 8 Visualization of computed flow in the non-peridic case (Sugiyama et al. 2003).

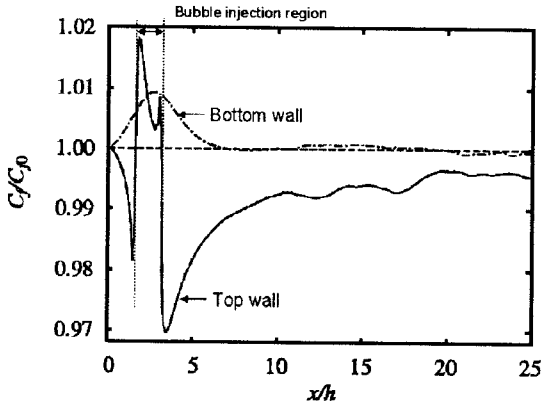

(a) Streamwise distribution of skin friction ratio

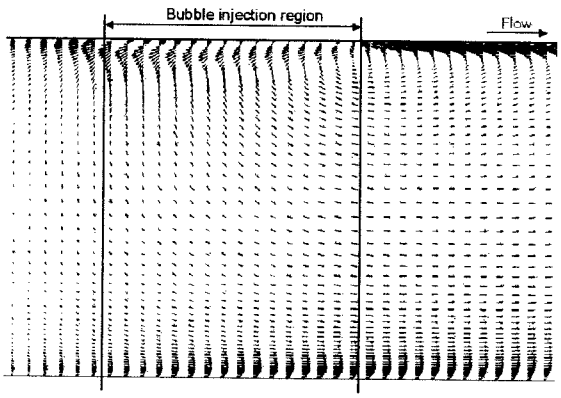

(b) Velocity difference between bubble and non-bubble conditions

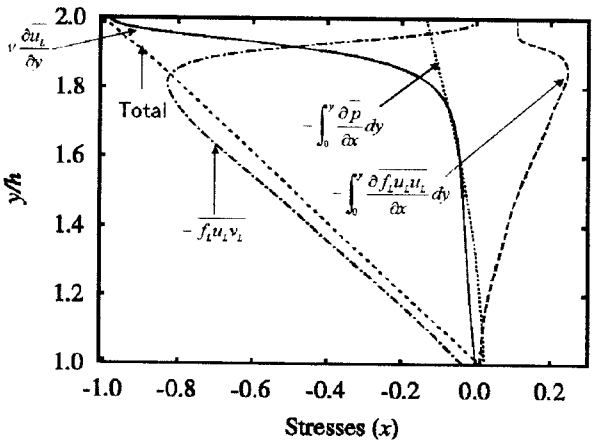

(c) Wall-normal distribution of the terms in eq.(4) at $0.79h$ location from the bubble injection region

Figure 9 Computed results of the non-periodic case (Sugiyama et al. 2003)

DISCUSSIONS ON SKIN FRICTION REDUCTION MECHANISMS OF MICROBUBBLES

Some possible mechanisms for the skin friction reduction effect of microbubbles are discussed.

Mechanism 1: Density effect

Among the possible mechanisms for the skin friction reduction by microbubbles, perhaps the most obvious is the density effect. When air bubbles are present, the density of the mixture decreases, and according to the shear stress representation

$$\tau = \mu \frac{\partial \overline{U}}{\partial y} - \rho \overline{UV} \tag{5}$$

the second term i.e. the Reynolds stress term decreases because ρ decreases. The liquid surface area, through which the first term acts, also decreases. The well-known phenomenon that significant skin friction reduction is obtained when bubbles are clustered near a solid wall supports this mechanism.

This effect is independent of the bubble size. But, in case the wall surface is horizontal and facing downward, i.e. the so-called "plate-on-top" condition (Merkle and Deutsch 1990), larger bubbles will have longer persistence in skin friction reduction because of larger buoyancy effect. This combination of the density effect and the buoyancy effect also explains the longer persistence at smaller flow speeds observed in the 50m-long flat plate test carried out in a towing tank (Takahashi et al. 2001).

Mechanism 2: Increase of effective viscosity

It has been theoretically and experimentally shown by many researchers that small bubbles or particles in liquid increase the effective viscosity of the liquid (Legner 1984, Madavan et al. 1985, Marie 1987). Although the increase of effective viscosity increases the first term of eq. (5), if this effect decreases the second term more significantly, the shear stress τ decreases. Since this effect does not depend on the Reynolds number and the ratio of the second term to the first term increases with increasing Reynolds number, this effect is perhaps more significant at higher Reynolds numbers.

In order for this mechanism to work, bubbles must be small. In microbubble experiments, although the size of most bubbles is 0.5mm to 1mm in diameter, much smaller bubbles are also observed. So, there is a possibility that those much smaller bubbles contribute to this effect. If this effect is important in the skin friction reduction mechanism, there is a chance to increase the skin friction reduction without increasing the amount of injected air.

Mechanism 3: Turbulence modification effect

Fig. 5 shows an example of this effect. It shows that bubbles increase turbulence fluctuations but decrease the Reynolds shear stress, i.e., the correlation between the two

velocity fluctuation components becomes smaller with bubbles. It is not yet clear why this occurs. The information which will be obtained using the PTV/LIF/IST system shown in Fig.3 will help to solve this problem.

It is also not clear whether this effect is influenced by bubble size or not.

Effect of bubble size/deformation

In the discussions shown above, the effect of bubble size is frequently mentioned. But they stay mostly as hypotheses. One of the reasons is that experimentally it is extremely difficult to control the size of generate bubbles without changing the other conditions, or to generate bubbles of uniform size. There are some trials in this respect. Moriguchi and Kato (2002) showed that the change of bubble size from 0.5mm to 2.0mm diameter does not influence the reduction effect. This range of bubble size is rather limited. Similar studies should be carried out on much smaller bubbles. The bubble generation technique is already available. For example Kawamura et al. generated bubbles of diameter 20 to 40 μm using a foaming technique.

ACKNOWLEDGEMENT

This study is funded by the Ministry of Education, Culture, Sports, Science and Technology, as a part of the research project "The Smart Control of Turbulence ; A Millennium Challenge for Innovative Thermal and Fluids Systems".

REFERENCES

Dean, R.B., 1978 "Reynolds number dependence of skin friction and other bulk flow variables in two-dimensional rectangular duct flow", J. of Fluids Engineering, 100, pp.215-223.

Kanai, T., Takekuma, K., Sato, K., Takahasi, K., and Yamaguchi, S. 2001, "Evaluation of CO2 Dissolution Contained in Marine Exhaust Gas Bubbles and Reduction of Ship's Frictional Resistance", J. of Soc. Naval Architects, Japan, vol.190, pp.305-317 (in Japanese).

Kasagi, N. and Kodama, Y. 2000 :Web site for the Center for Smart Control of Turbulence. http://www.turbulence-control.gr.jp /index_e.html

Kawamura, T., Kakugawa, A., Kodama, Y., Moriguchi, Y. and Kato, H., 2002, "Controlling the Size of Microbubbles for Drag Reduction," Proceedings of the 3rd Symp. on Smart Control of Turbulence, pp.121-128. Also see http://www.turbulence-control.gr.jp /index_e.html

Kitagawa, A., Fujiwara, A., Hishida, K., Kakugawa, A., and Kodama, Y., 2003, "Turbulence structures of microbubble flow measured by PIV/PTV and LIF techniques", 4th Symp. on Smart Control of Turbulence, pp.131-140.

Kodama, Y., Kakugawa, A., Takahashi, T. and Kawashima, H., 2000, "Experimental study on microbubbles and their applicability to ships for skin friction reduction.", Int. J. of Heat and Fluid Flow vol.21.

Kodama, Y., Kakugawa, A., Takahashi, T., Nagaya, S., Sugiyama, K. and SR239 Committee, 2002a "Microbubbles: Drag Reduction Mechanism and Applicability to Ships", 24th Symposium on Naval Hydrodynamics, Fukuoka, JAPAN.

Kodama, Y., Kakugawa, A., Takahashi, T., Ishikawa, S., Kawakita, C., Kanai, T., Toda, Y., Kato, H., Ikemoto, A., Yamashita, K., and Nagamatsu, T., 2002b, " A Full-scale Experiment on Micro-bubbles for Skin Friction Reduction Using SEIUN MARU Part 1 : The Preparatory Study", J. of the Society of Naval Architects of Japan, vol.192, pp.1-14 (in Japanese).

Legner, H.H., 1984, A simple model for gas bubble drag reduction, Phys. Fluids 27 (12) pp.2788-2790.

Madavan, N.K., Merkle, C. and Deutsch, S., 1985, "Numerical Investigations into the Mechanisms of Microbubble Drag Reduction", Journal of Fluids Engineering Vol.107, pp.370-377.

Marie, J.L., 1987, A Simple Analytical Formulation for Microbubble Drag Reduction, PhysicoChemical Hydrodynamics Vol.8, No.2, pp.213-220.

McCormick, M.E. and Bhattacharyya, R., 1973, "Drag Reduction of a Submersible Hull by Electrolysis", Naval Engineers Journal, Vol.85, No.2, pp. 11-16.

Merkle, C. and Deutsch, S., 1990 "Drag Reduction in Liquid Boundary Layers by Gas Injection", Progress in Astronautics and Aeronautics vol.123, AIAA, pp.351-412.

Moriguchi, Y. and Kato, H. 2002 "Influence of microbubble diameter and bubble distribution on frictional resistance reduction by microbubbles," J. of Marine Science and Technology vol.7, No.2, pp.79-85.

Nagamatsu, T., Kodama, Y., Kakugawa, A., Takai, M., Murakami, K., Ishikawa, S., Kamiirisa, H., Ogiwara, S., Yoshida, Y., Suzuki, T., Toda, Y., Kato, H., Ikemoto, A., Yamatani, S., Imo, S., and Yamashita, K., 2002, " A Full-scale Experiment on Microbubbles for Skin Friction Reduction Using SEIUN MARU Part 2 : The Full-scale Experiment", J. of the Society of Naval Architects of Japan, vol.192, pp.15-28 (in Japanese).

Nagaya, S., Hishida, K., Kodama, Y., and Kakugawa, A., 2002, "Measurements for Turbulent Channel Flow Containing Microbubbles Using PIV/LIF Technique", The 24th ASME International Mechanical Engineering Congress, IMECE2002-33791.

Sugiyama, K., Kawamura, T., Takagi, S., and Matsumoto, Y., 2003, "Numerical Simulation of Transient Microbubble Flow", 4th Symp. on Smart Control of Turbulence, pp.51-60.

Takahashi, T., Kakugawa, A., Kodama, Y., and Makino, M. 2001, "Experimental study on drag reduction by microbubbles using a 50m-long flat plate ship" TSFP-2, 2nd Int. Symp. on Turbulence and Shear Flow Phenomena, Vol.1, pp.175-180.

Takahashi, T., Kakugawa, A., Makino, M., and Kodama, Y. 2003, "Experimental Study on Scale Effect of Drag Reduction by Microbubbles", Journal of the Kansai Society of Naval Architects, Japan, Vol.239 (in Japanese).

Watanabe, O., Masuko, A., and Shirose, Y. 1998, "Measurements of Drag Reduction by Microbubbles Using Very Long Ship Models", J. of Soc. Naval Architects, Japan, vol.183, pp.53-63 (in Japanese).

Xu, J., Maxey, M.R. and Karniadakis, G.E., 2002, "DNS of turbulent drag reduction using micro-bubbles", J. Fluid Mech. 468, 271-281.